

# EVALUATION METHOD FOR ALLOWABLE SHORT-TERM FLEXURAL STRENGTH AND YIELD STRENGTH OF CONCRETE-FILLED STEEL TUBULAR COLUMNS

TAKASHI FUJINAGA<sup>1</sup> and TOMOYA KAWABATA<sup>2</sup>

<sup>1</sup>Research Center for Urban Safety and Security, Kobe University, Kobe, Japan

<sup>2</sup>Graduate School of Engineering, Kobe University, Kobe, Japan

According to the Recommendations for Design and Construction of Concrete Filled Steel Tubular Structures from Architectural Institute of Japan, the allowable short-term flexural strength (ASFS) can be used as the yield strength for the restoring force characteristics model of concrete-filled steel tube (CFST) members. Therefore, it is necessary to examine whether the ASFS can be appropriate as an alternative for the yield strength. Furthermore, as the ASFS is typically calculated using the superposition method, the value of the deformation at the superposed strength cannot be evaluated. To address these issues, in this study, numerical analysis was conducted on the moment–curvature relation of CFST column sections using the finite fiber method. The characteristics of the point of ASFS and evaluation method for flexural yield strength in a broad sense were examined using the slope factor and strength satisfaction factor methods. The corresponding slope factor is larger than the value (1/3) that is generally used for the yield strength definition. Therefore, using the ASFS is as the yield strength of the CFST section is reasonable. Additionally, the formula for the curvature at the ASFS was also proposed.

*Keywords:* Concrete-filled steel tube, Numerical analysis, Stress-strain relationship, Slope factor, Strength satisfaction factor.

## 1 INTRODUCTION

In Japan, it is common to reference the Recommendations for Design and Construction of Concrete Filled Steel Tubular Structures by the Architectural Institute of Japan (AIJ 2008) when designing concrete-filled steel tube (CFST) structure buildings. Based on these recommendations, the allowable short-term flexural strength (ASFS) is used as the yield flexural strength for the restoring force characteristics model of CFST members. However, it is unclear whether doing so is appropriate from safety perspective and, thus, we believe it necessary to examine the validity of this practice. Furthermore, the ASFS of a CFST section is calculated easily using the superposition of the strength of the steel section and that of the concrete section. However, this method is not deformation-based; therefore, it cannot evaluate the value of the deformation and/or the curvature at the calculated superposed strength.

## 2 NUMERICAL ANALYSIS OF CFST SECTION

### 2.1 Outline of Numerical Analysis

A numerical analysis was conducted to determine the bending moment–curvature relation using the so-called finite fiber method. The following assumptions were adopted: (1) the plane section remains plane after bending; (2) the tensile strength of concrete is ignored; (3) the shear deformation is ignored; and (4) the curvature is increased monotonically.

The analysis targets were rectangular and circular CFST sections. The numerical analysis parameters are as follows: the depth-to-thickness ratios of the rectangular steel tubes are  $B/t = 20, 30, \text{ and } 40$ , and the diameter-to-thickness ratios of the circular steel tubes are  $D/t = 30, 45, \text{ and } 60$ ; the yield stresses of steel,  $f_y$ , are 300 MPa and 600 MPa, respectively; the compressive strength of the filled-concrete,  $f_c'$ , are 30 MPa, 60 MPa, and 90 MPa, respectively. However, parameter combinations such as  $f_y = 300$  MPa and  $f_c' = 90$  MPa, and  $f_y = 600$  MPa and  $f_c' = 30$  MPa are not realistic materials strength of CFST sections, and are therefore excluded from this analysis. Additionally, the axial force ratio,  $n$ , are 0.1, 0.2, 0.3, 0.4, 0.5, and 0.6. The cases of axial force ratio 0.6 and the axial force ratio of 0.5 (partially) are beyond the axial force ratio limit ( $N_l$ ) of the AIJ CFST recommendations ( $N_l = 1/3 \rho A f_c' + 2/3 \rho_s A f_y$ ) (AIJ 2008). As the curvature increment was monotonic, the effect of the repetition was not considered.

### 2.2 Stress–Strain Relationship of Rectangular CFST Section

#### 2.2.1 Stress–strain relationship of steel

For the computation of the rectangular CFST section behavior, the stress–strain relation on the compression side of the steel tube (Figure 1) was based on the model by Zhao *et al.* (2017). The model is based on a significant amount of experimental data from static compression tests. However, the strain at the characteristic point in the stress descending part,  $\varepsilon_{res}$ , is modified as in Eq. (1) (Sakurai *et al.* 2018) to consider the difference between the experimental measurement length and the length of the plastic region.

For the tension side of the steel tube, the perfect elastic-plastic model is used. The tensile yield strength is multiplied by 1.08 in consideration of the effect of the biaxial stress state.

$$\varepsilon_{res} = 0.12 - 2\varepsilon_{sm} \quad (1)$$

where  $\varepsilon_{sm}$  is the compressive side steel strain at maximum stress.

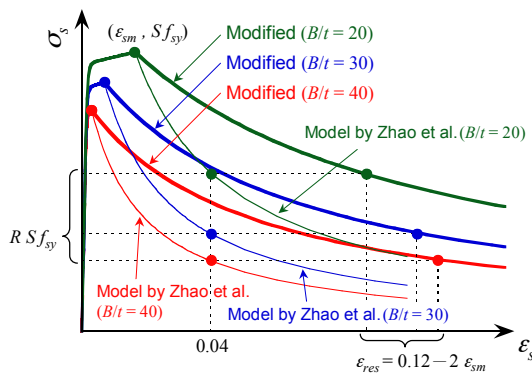


Figure 1. Stress–strain model for compressive range of square steel pipe.

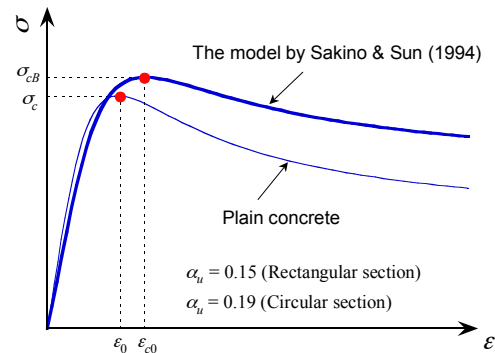


Figure 2. Stress–strain model of concrete.

### 2.2.2 Stress–strain relationship of concrete

The stress–strain relation of filled-concrete (see Figure 2) was based on the model by Sakino and Sun (1994). In the model, the constant value of the downslope factor after the maximum strength is set as 2.25, in consideration of the strain gradient effect in the section (Tian *et al.* 1997). Here, for the computation of the rectangular CFST behavior, the lateral pressure to the steel tube is calculated by Eq. (2), and the ratio of the circumferential stress of the steel tube is assumed to be  $\alpha_u = 0.15$ . This value was obtained to predict the average maximum compressive strength from the test data of the rectangular CFST stub columns (Sakurai 2019).

$$\sigma_{re} = \frac{1}{2} \rho_h \frac{t}{d} \alpha_u \cdot f_{sy} \quad (2)$$

### 2.3 Stress–Strain Relationship of Circular CFST Section

No combinations and applications of the stress–strain relation model of circular steel tube exist in literature so far for the calculation of the circular CFST section behavior. Simple models were used in this study for the examination of the circular CFST section behavior. The stress-strain relationship of steel is based on a perfect elastic–plastic model. It was assumed that a circumferential stress of  $0.19 f_y$  acted on the steel tube, the yield stress in the biaxial tensile was  $1.08 f_y$ , and the yield stress in the compression side was  $0.89 f_y$  (AIJ 2008).

The model by Sakino and Sun (1994) was used for the stress–strain relation of filled concrete. To account for the effect of the strain gradient in the section, the downslope factor after the peak was set as 2.25 (Tian *et al.* 1997), and the ratio of the circumferential stress of the steel tube was assumed to be  $\alpha_u = 0.19$  (AIJ 2008). The lateral pressure on the steel tube can be calculated by Eq. (3) (Sakino *et al.* 2004).

$$\sigma_{re} = \frac{4.1}{23} \cdot \frac{2t}{d} \alpha_u \cdot f_y \quad (3)$$

## 3 RESULTS AND DISCUSSION

### 3.1 Comparison of Allowable Short-Term Strength and Strength at Characteristic Points

The ASFS,  $M_a$ , is compared with the strength at characteristic point, which that defines the general yield strength by utilizing a generally used slope factor method and to investigate the simpler strength satisfaction factor method. The characteristic points examined in this study were as follows: (A) the point where the tangent rigidity decreased to 1/3, 0.4, 0.5, and 0.6 times its initial rigidity in the moment–curvature relation (the slope factor method), and (B) the point where the bending moment reached 0.6 and 0.7 times the maximum flexural strength (the strength satisfaction factor method).

#### 3.1.1 Comparison with flexural strength using strength satisfaction factor

Figure 3 shows the relationship between the axial force ratio,  $n$ , and the flexural strength ratio determined to satisfy the factor on the basis of maximum flexural strength and ASFS,  $kM_{\max} / M_a$ . As shown in the graphs, the larger the axial force ratio is, the larger the increase in flexural strength ratio. The distribution trend is rising to the right. Additionally, the strength ratio dispersion tends to be large when the depth-to-thickness and axial force ratios are large. Thus, the correspondence of the flexural strength determined by the strength satisfaction factor and ASFS is not good, and it is not appropriate to predict ASFS using the strength satisfaction factor.

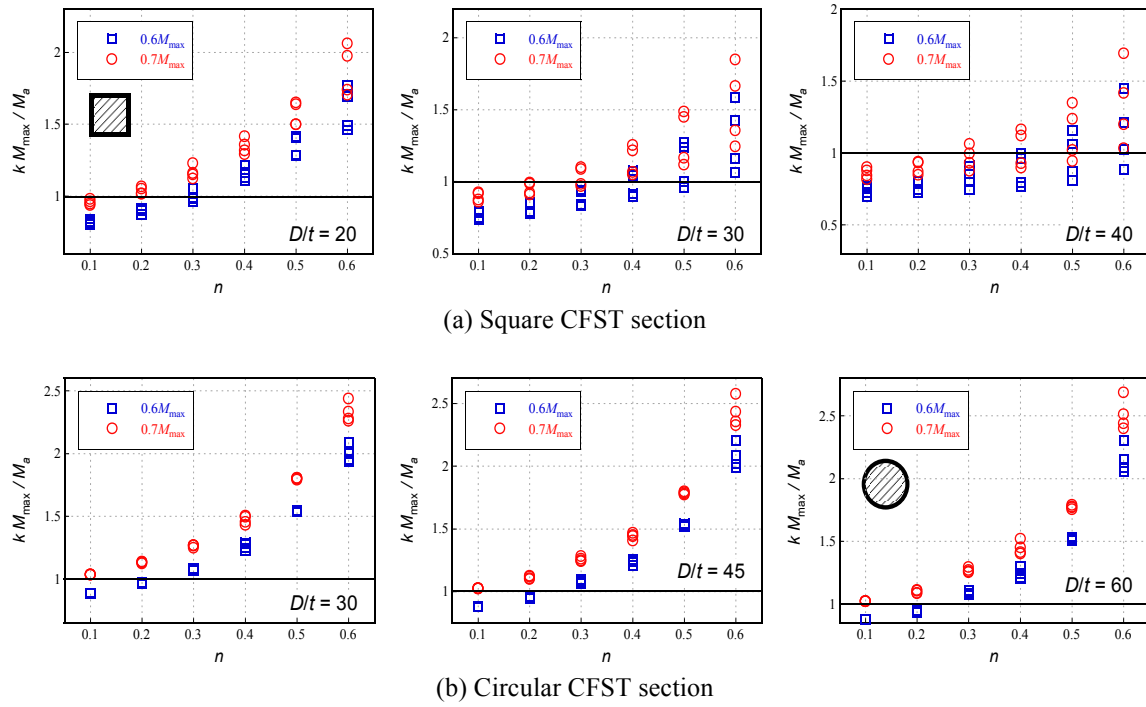


Figure 3. Comparison between ASFS and flexural strength using strength satisfaction factor.

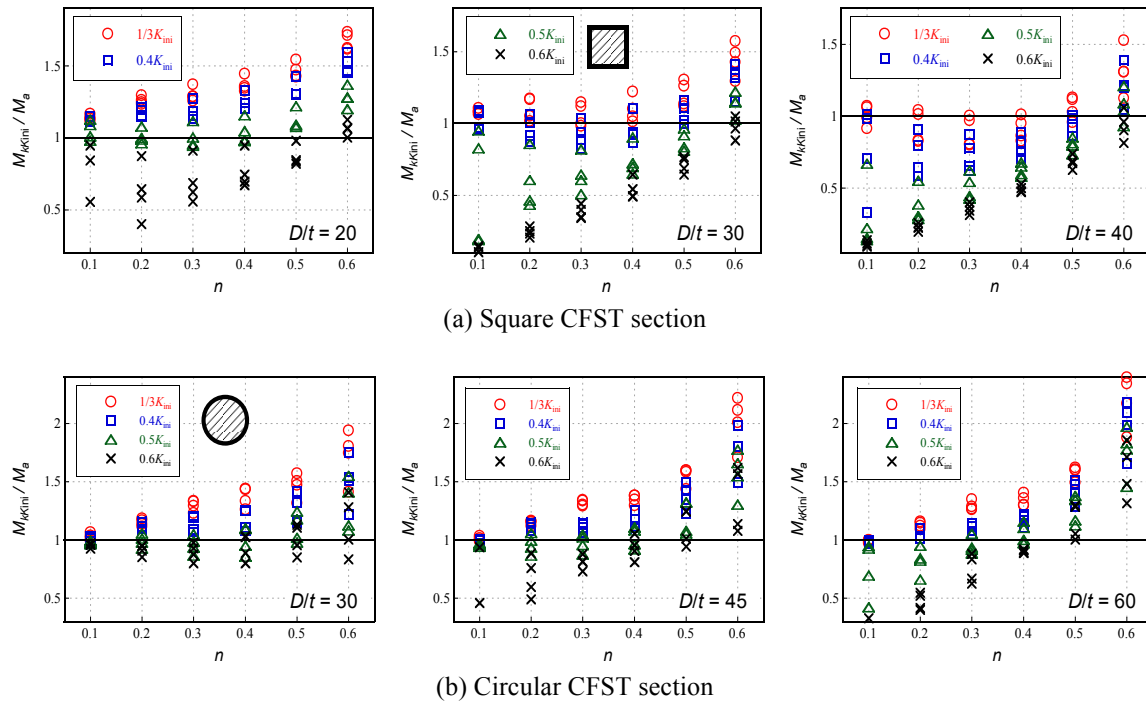


Figure 4. Comparison between ASFS and flexural strength using slope factor.

### 3.1.2 Comparison with flexural strength using slope factor

Figure 4 shows the relationship between the axial force ratio,  $n$ , and the flexural strength ratio where the tangent rigidity decreased to the slope factor and ASFS,  $M_{kkini}/M_a$ . As shown in the figures, an appropriate factor exists, when ASFS is predicted using slope factor, where the strength ratio becomes relatively uniform regardless of the axial force ratio. The strength ratio distribution tendency is increasing to the right when the axial force ratio is large. However, the cases with the axial force ratio of 0.6 and the axial load ratio 0.5 (partially) are outside the AIJ's recommended range of use for CFST sections.

In the case of the rectangular CFST section, at a depth-to-thickness ratio of 20, the slope factor where the strength ratio becomes uniform is 0.5. If the depth-to-thickness ratio becomes larger, the strength using a slope factor of 1/3, generally used for yield strength evaluation, predicts ASFS fairly accurately. In the case of the circular CFST section, the slope factor where the strength ratio becomes uniform and almost 1.0 is 0.5 for a diameter-to-thickness ratio of 30. The appropriate slope factor is 0.4–0.5 in the case of a diameter-to-thickness ratio of 45, and 0.4 in the case of a diameter-to-thickness ratio of 60.

The influence of the axial force ratio is minor on the ratio of the flexural strength to ASFS. The slope factor where the strength factor is close to 1.0 is approximately equal to a commonly used factor of 1/3 or a slightly larger value. Therefore, it can be inferred that it is appropriate to use ASFS as a general yield flexural strength and is a safe side judgement in most case.

### 3.2 Curvature at Allowable Short-Term Flexural Strength

Figure 5 depicts the relationship between the axial force ratio and the curvature at the ASFS. The value of the curvature is normalized by multiplying the depth or diameter of the section. As shown in the plots, the values of curvature at ASFS depend on the value of the yield stress of steel and are in an almost linear relation. The influence of the concrete strength is small. Some differences exist in the case when the yield stress of steel is  $f_y = 600$  MPa; however, this is not owing to the influence of the concrete strength but the influence of the depth-to-thickness and diameter-to-thickness ratios. The curvature at ASFS tends to be small when the depth-to-thickness and diameter-to-thickness ratios are large.

The curvature corresponding to the ASFS of rectangular and circular CFST sections  $\phi_{Ma} D$  can be expressed by the approximation equations in Eq. (4).

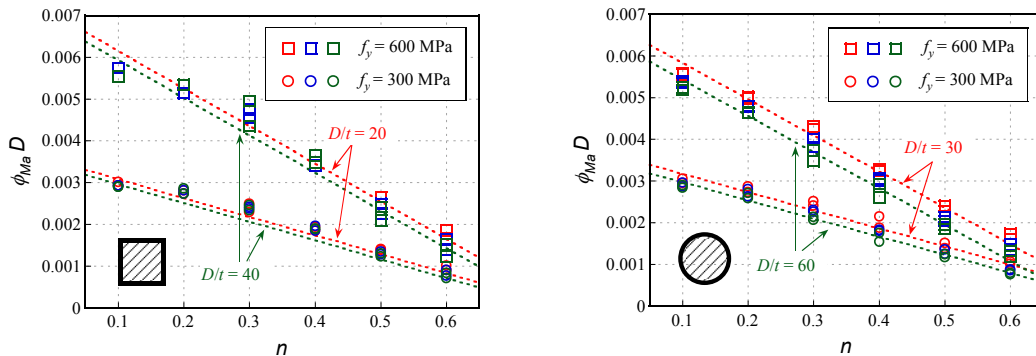


Figure 5. Curvature at the allowable short-term flexural strength.

$$\begin{aligned} \phi_{Ma} D &= \left( -1.5n + 1.1 + 1.5 \frac{t}{D} \right) f_y \cdot 10^{-5} && \text{for Rectangular CFST} \\ \phi_{Ma} D &= \left( -1.45n + 0.9 + 4 \frac{t}{D} \right) f_y \cdot 10^{-5} + 0.0005 && \text{for Circular CFST} \end{aligned} \quad (4)$$

Figure 6 shows the comparison between the numerically obtained curvature at ASFS and the value of the proposed approximate formulae. Within the range of the parameters considered in this study, the proposed formulae accurately predict the numerically obtained curvature at ASFS.

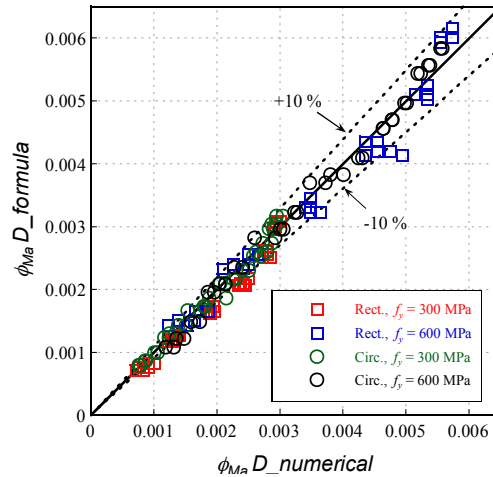


Figure 6. Comparison with proposed formulae and curvature at the ASFS.

#### 4 CONCLUSIONS

These results numerically suggest that it is appropriate to use the ASFS as an alternative to the yield strength of the concrete-filled steel tubular section. Additionally, the formula for the curvature corresponding to the ASFS was proposed. The yield strength point of the moment-curvature relation can be defined using ASFS and its curvature.

#### References

- Architectural Institute of Japan (AIJ), *Recommendations for Design and Construction of Concrete Filled Steel Tubular Structures*, 2<sup>nd</sup> Edition, 2008.
- Architectural Institute of Japan, *Design Standard for Composite Structures*, January, 2014.
- Sakino, K., and Sun, Y., *Stress-strain Curve of Concrete Confined by Rectilinear Hoop*, Journal of Structural and Construction Engineering (Transactions of AIJ), No.461, 95-104, July, 1994.
- Sakino, K., Nakahara, H., Morino, S., and Nishiyama, I., *Behavior of Centrally Loaded Concrete-Filled Steel-Tube Short Columns*, Journal of Structural Engineering ASCE, Vol.130(2), 180-188, February, 2004.
- Sakurai, H., Fujinaga, T., Takeuchi, T., and Sun, Y., *Analytical Study on Square CFT Beam-columns Considering the Height of Critical Section*, Proceedings of Constructional Steel, Vol.26, 36-42, November, 2018.
- Sakurai, H., *Analytical Study on Square CFT Beam-columns' Hysteresis*, Master's thesis Kobe University, February, 2019.
- Tian, F., Sakino, K., and Sun, Y., *Effect of Strain Gradient on the Flexural Behavior of Confined R/C Columns*, Journal of Structural Engineering, Vol.43B, 191-198, March, 1997.
- Zhao, H., Sun, Y., Takeuchi, T., and Zhao, S., *Comprehensive stress-strain model of square steel tube stub columns under compression*, Engineering Structure 131, 503-512, 2017.